Component Level Fragility Estimation for Vertically Irregular Reinforced Concrete Frames

Trishna Choudhury & Hemant B. Kaushik

Check for updates
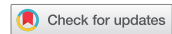
Component Level Fragility Estimation for Vertically Irregular Reinforced Concrete Frames

Trishna Choudhury and Hemant B. Kaushik ⓘD

Department of Civil Engineering, Indian Institute of Technology Guwahati, Guwahati, India

ABSTRACT

Seismic fragility functions are essential for performance-based seismic design of structures. Global demand parameters, such as peak roof displacement or maximum drift over the height of the building, are commonly used to estimate seismic fragility. However, in case of buildings with vertical irregularities, the global demand parameters may not suffice since maximum demand in such building is mostly concentrated at the level of irregularity. The current study focuses on one of the most common forms of vertically irregular reinforced concrete (RC) buildings, known as open ground story buildings, where irregularity lies at the ground story. Nonlinear dynamic analyses of RC frames subjected to a number of ground motions, each scaled-up for different PGA, are carried out to estimate the component level and global drift demands, also known as engineering demand parameters (EDPs). Seismic fragilities developed for the frames based on both the component and global EDPs are presented. Finally, the importance of component-based fragilities for estimation of seismic fragility of irregular frames is emphasized. The component level EDP-based fragility is found to be effective in predicting the actual damage scenarios in such buildings observed during past earthquakes.

Introduction

Reinforced Concrete (RC) buildings are the most common type of construction typology existing worldwide. RC buildings with masonry infill walls have undergone varying degree of damage during past earthquakes; therefore, seismic fragility assessment of such buildings becomes necessary to predict its damageability. RC frames with irregular distribution of infills are seismically even more vulnerable. For example, open ground story buildings are vertically irregular buildings with no infills in the ground story. As discussed later, such buildings undergo large lateral deformation in the ground story, resulting in excessive ductility demand from ground story columns leading to their eventual failure. The present study investigates the existing seismic fragility assessment methodologies with respect to different engineering demand parameters (EDPs) for RC frames with and without vertical irregularities (soft story effect). EDPs are structural response quantities that can be used to predict damage to structural and nonstructural components and systems [Whittaker *et al.*, 2004]. The most common global EDP considered in a large-

---

scale fragility assessment of building stock includes peak roof or top story displacement or maximum inter-story drift over the height of the building. Here, the global displacement or drift response of the building is entirely defined by the top story displacement assuming the first modal displacement pattern as dominant. However, such a methodology is insufficient to describe exactly the failure mechanism in buildings, particularly in case of irregular frames, such as open ground story (OGS) frames, where the failure is mostly concentrated at the level of irregularity. OGS columns lack adequate ductility capacity, stiffness, and strength needed to resist the high demand of story shear. This leads to an undesirable column-sway failure mechanism in OGS buildings subjected to earthquake excitations, in which failure occurs mostly in the columns of the ground story. In contrast, the infills present in the upper stories restrain the deformation of the upper story, and thus, little damage is incurred in the upper storys of such buildings. The vulnerability of the open ground story frames was observed by Mondal and Tesfamariam [2014] who reported that the infill thickness and vertical irregularity have significant influence on the response of RC frames. Similarly, the higher seismic vulnerability of vertically irregular masonry infilled frames was also observed in several past studies [e.g., Dolšek and Fajfar, 2001; Yuen and Kuang, 2015; Choudhury and Kaushik, 2018; Aschheim *et al.*, 2000; Kaushik and Jain, 2007].

Existing fragility assessment procedures, for example, HAZUS [2013], require displacement thresholds to be defined for a frame-type specifying the limiting displacement capacity of the frame at various damage levels. Several documents and literature suggest such limiting displacement capacity values for different frame typologies. HAZUS defines these thresholds based on average inter-story drift ratio, which can be converted to corresponding top story displacement by multiplying with the height of the building, thus showing a first mode deformation profile, with highest displacement at the top. This procedure provides a good estimate of fragility for regular frames, but distort the true fragility of irregular frames, such as, an OGS frame.

In order to specify the amount of structural and nonstructural damage to structures, EDPs are identified. Several building codes and articles [FEMA, 2000; Whittaker *et al.*, 2004; Ramamoorthy *et al.*, 2006; Jalayer and Cornell, 2009; HAZUS, 2013; Liu *et al.*, 2016] suggest maximum roof displacement or drift as a sufficient EDP to predict the building performance, and hence it's fragility. For all structural framing systems, inter-story drift is one of the traditionally used EDP, however, this is considered only at the top or roof level of the building frame. Contemporary probabilistic seismic analysis mainly focusses on global EDPs, owing to the high computational effort required for monitoring component level EDPs. Instead, a few researchers [Ruiz-García and Miranda, 2010] considered residual (permanent) drift demand as an efficient EDP for design of new buildings and for seismic assessment of buildings based on field observations. Prior to this, Ruiz-García and Miranda [2006] showed height-wise distribution of residual lateral deformation demands in multistory degree of freedom systems.

Other works, such as Kazantzi and Vamvatsikos [2015] recommended the use of story level EDPs (peak inter-story drift ratio and peak floor acceleration at each floor) as adequate for assessing the structural and nonstructural losses. Similarly, Freddi *et al.* [2017] highlighted that the global demand parameters, such as maximum displacement or drift over the height of the building is insufficient in predicting the response of structures that correlates well with the expected damage or failure pattern in low ductile

RC frames. Ellingwood *et al.* [2007] suggested use of maximum inter-story drift angle as the demand variable due to its capability to provide an insight into the structural or local collapse. Another study on multistory frames by Bai *et al.* [2011] developed probabilistic seismic demand models based on inter-story drift at each story. It was concluded that the traditional demand model using the overall maximum inter-story drift cannot capture the contribution from the story responses.

Previous studies suggested various EDPs for fragility assessment of multistoried frames; however, such categorized EDPs are not available in the literature for irregular buildings. Hence, a component level fragility analysis, with local demand parameters, is carried out in the present study to estimate the realistic fragility of vertically irregular buildings. The present study clearly brings out the importance of a component level EDP in fragility estimation of vertically irregular building frames with a focus on open ground story frames. The roof level displacement as EDP for fragility estimation may not always depict the true behavior of the frames. Instead, a component level EDP may be a better alternative for realistic seismic fragility assessment of vertically irregular structures. For this purpose, an internal frame (Fig. 1) of a three-bay, four-story (3B-4S) RC building, designed and detailed for the highest seismic zone as per the relevant Indian Standards [BIS, 2002], is considered. Three different structural configurations representing both regular and irregular frames are considered for the 3B-4S RC frame as listed below:

(a) Bare Frame (BF): Masonry infill walls are not provided in any story (regular frame).
(b) Open Ground Story (OGS) Frame: Masonry infill walls are provided in all the stories except the ground story (vertically irregular frame).
(c) Fully Infilled (FI) frame: Masonry infill walls are provided in all the storys (regular frame).
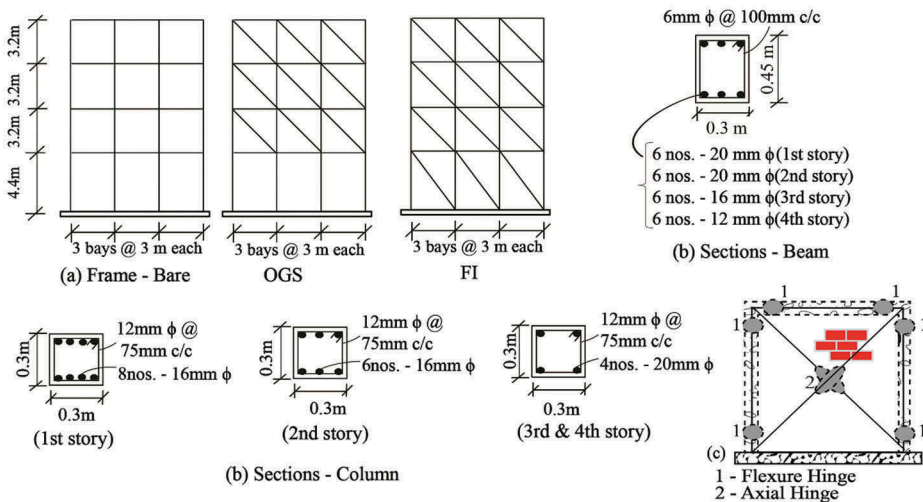
Figure 1. (a) Structural frame – bare, OGS, and FI frame (b) Sectional details - beams (0.3 m x 0.45 m) and columns (0.3 m x 0.3 m). Here, φ is diameter of bar, and c/c is center to center distance (c) RC frame and equivalent strut model with lumped plasticity.

Nonlinear dynamic analyses of the frames subjected to realistic ground motions are carried out in order to obtain the displacement demands on the frames at each story level. The primary objective of the study is to bring out a favorable engineering demand parameter that realistically defines the failure as well as the seismic fragility for RC frames with vertical irregularity.

Analytical modeling and nonlinear analyses of the frames

Nonlinear (NL) static and dynamic analyses of the frames are carried out to investigate the frame behavior under earthquake excitations. NL dynamic analyses are carried out using time-history analysis, which involves time-step-by-time-step evaluation of the building response. The peak inter-story drift (ISD) demands and maximum story displacement for different intensity of considered ground motions are obtained at each floor level of the frame and used as EDP for seismic fragility estimation.

Generic buildings and analytical modeling

Three different building typologies are considered for seismic analysis, namely, Open Ground Story (OGS) frame, Fully Infilled (FI) frame and Bare Frame (BF), and modeled in SAP 2000 [CSI, 2015] for nonlinear analyses (Fig. 1). The number of bays and stories in the frame, material properties, and reinforcement detailing are decided based on the commonly constructed apartment buildings in India and many other countries. For the mid-rise buildings, the present configuration, that is, three bay four story (3B-4S) can be considered as a median case building. The conclusions obtained for the 3B-4S representative sample are equally applicable to other mid-rise building frames. Though ductile detailing was provided in the RC frame members, the frame was designed as a weak column-strong beam frame system to reflect the current design practice adopted by designers in India as well as in many other countries [Kaushik et al., 2009]. The bare frame is modeled as per general design criteria of considering only the weight of infills in the frame members. For the OGS frame, stiffness and strength of masonry infills are considered in the upper stories; however, the ground story of the frame is kept open, that is, without masonry infills. The fully infilled (FI) frames are provided with masonry infills at all stories uniformly. Thus, both the strength and stiffness of masonry infill wall are considered while modeling for nonlinear analyses of FI frame.

Sectional details of various members of the frame are shown in Fig. 1(b). The frames are fixed at the base of ground story columns. Beams and columns are modeled as line elements with concentrated plasticity defined using fiber sections. The masonry infill walls are modeled as single equivalent diagonal strut of thickness same as the wall thickness [Kaushik et al., 2009]. Length of the strut is determined as diagonal length of the infill panels and width is considered as one-fourth of the diagonal length of the struts. The beams and columns of the frames are detailed to exhibit ductile response. Therefore, shear failure of the columns is not expected and not considered in the present study. There is a possibility of shear failure of the columns due to frame-infill interaction. However, this is a complex phenomenon, which is not taken care of by the simplified diagonal strut modeling used in the present study. The masonry infill panels can fail in several failure modes under seismic action, for example, diagonal compression, crushing in the corners in

contact with the frame, sliding shear along horizontal joints and diagonal tension. The present study, however, considers only the diagonal compression as the failure mode in infill panels that can be captured by the simplified equivalent diagonal strut model.

The natural period of vibration for the first and second mode of the BF, OGS, and FI frames are listed in Table 1. There is a large difference in the natural time period of the FI frames as compared to the bare or OGS frames due to the presence of infills in the ground story that imparts large stiffness to the frame and reduces the time period.

Material modeling

The materials considered in the analytical models are concrete, reinforcing steel, and masonry infill. The compressive cube strength of concrete is considered as 25 MPa (Elastic Modulus: 25,000 MPa) and the reinforcing bars have expected yield stress of 450 MPa (Elastic Modulus: 200 GPa). Mander's model [Mander et al., 1988] is used to characterize the stress-strain curve of concrete. Idealized stress-strain model proposed by Kaushik et al. [2007] is used to model the material nonlinearity in masonry considering masonry prism strength of 4.1 MPa and elastic modulus of 2255 MPa (Fig. 2).

The Mander model gives the stress-strain envelop in each of the concrete fibers (discussed later) in a section, however, its hysteresis characteristics, that is, the strength and stiffness degradation for every loading and unloading, is defined by the Takeda hysteresis model. The Takeda model [Takeda et al., 1970] shown in Fig. 3(a) includes stiffness changes at flexural

Table 1. Table showing dynamic properties of the frames considered.

Frame	Mode1		Mode2		Floor mass (Tonne)			
	T_N	Γ	T_N	Γ	Floor1	Floor 2	Floor 3	Floor 4
Bare frame	0.97	0.94	0.30	0.04	43.7	43.7	43.7	32.9
OGS frame	0.78	0.98	0.11	0.001				
FI frame	0.25	0.87	0.09	0.11				

T_N = Natural period of vibration, Γ = modal mass participation ratio
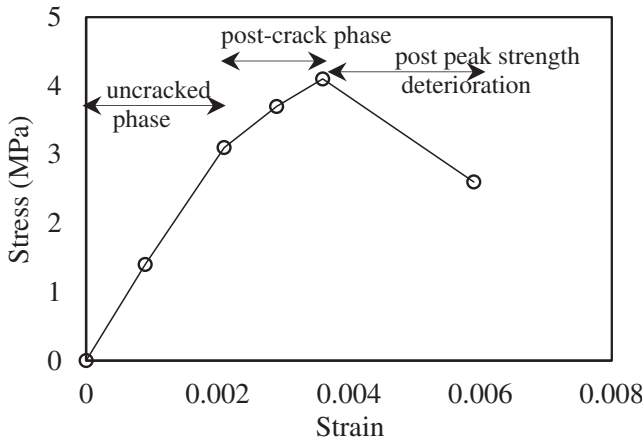
Figure 2. Idealized monotonic stress strain model for weak masonry infill [Kaushik et al., 2007].
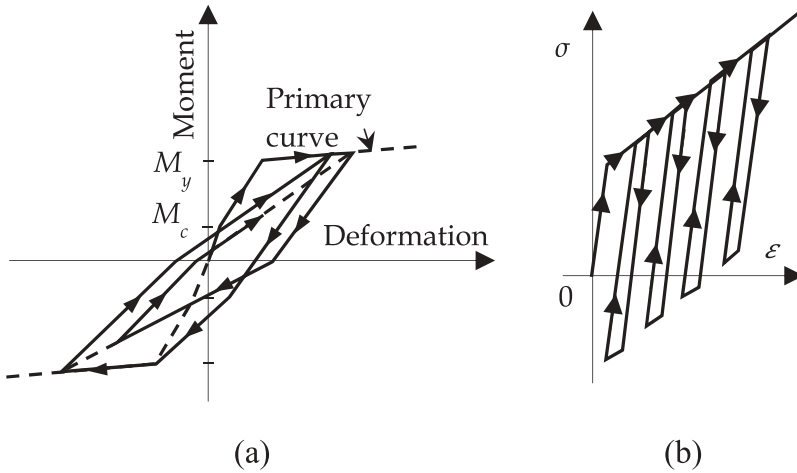
Figure 3. (a) Force-deformation relationship of Takeda's degrading stiffness model [Takeda *et al.*, 1970], (b) Typical kinematic hysteresis model for reinforcing bars [Hahn *et al.*, 1990].

cracking and yielding, and also strain-hardening characteristics. The Takeda model simulates dominantly the flexural behavior. The model has a tri-linear envelope curve and is designed to dissipate energy even at low cycles once the cracking point has been exceeded.

Figure 3(b) shows a typical kinematic hysteresis model used for reinforcing bars [Hahn *et al.*, 1990]. This model is based on kinematic hardening behavior that is commonly observed in metals. This model dissipates a significant amount of energy, and is appropriate for ductile materials. Upon unloading and reverse loading, the curve follows a path made of segments parallel to and of the same length, as the previously loaded segments and their opposite-direction counterparts until it rejoins the backbone curve when loading in the opposite direction.

Figure 4 shows the Pivot hysteretic model [Cavaleri and Di Trapani, 2014] used for equivalent strut for masonry infill. The points S_1, S_2, and S_3 on the compression envelope represent, respectively, the yield, the peak, and the restoring force corresponding to a
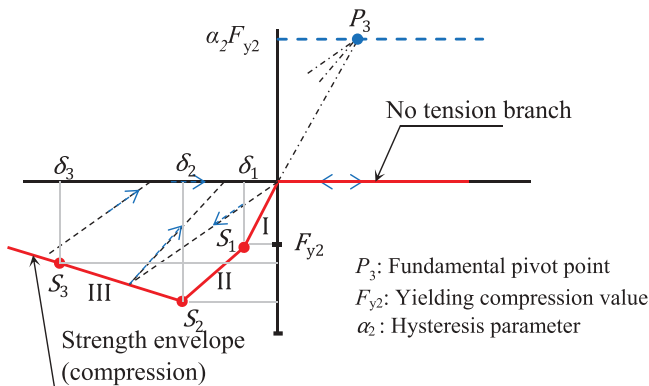
Figure 4. Hysteretic Pivot law particularization for the equivalent diagonal strut [Cavaleri and Di Trapani, 2014].

reduction of 30% of the peak strength. δ_1 and δ_2 are the yield and peak displacements, respectively, and δ_3 is the final displacement after softening. I, II, and III define the yielding, peak, and softening branches of the model. The Pivot model is based mainly on geometrical rules that define loading and unloading branches rather than analytical laws. This reduces not only the computational effort but also the number of hysteretic parameters involved. Moreover, the Pivot model has great flexibility in modeling unsymmetrical tension–compression behaviors, as in the case of infill equivalent struts.

When fiber hinges are used, the cross section is discretized into a series of axial fibers, which extend along the hinge length. Each of these fibers has a stress-strain relationship, and together these define the force-deformation and moment-rotation relationships for the frame section. Although the fiber hinge is computationally more intensive, it is used in the present analyses, since it gives more accurate results.

For the frames, first gravity load analysis, as a combination of dead and live loads (DL + 0.25×LL), is carried out before nonlinear dynamic analysis. P-delta effects are not included in the analyses as the frames are not expected to undergo large deformations. Rayleigh damping (C) is assumed based on a modal damping ratio of 5% [Wilson, 1996] and calculated using Eq. (1).

$$C = \alpha M + \beta K \tag{1}$$

where, α and β are scale factors calculated using Eq. (2).

$$\alpha = \frac{2(\xi_i \omega_j - \xi_j \omega_i)\omega_i \omega_j}{\omega_j^2 - \omega_i^2}, \quad \beta = \frac{2(\xi_j \omega_j - \xi_i \omega_i)}{\omega_j^2 - \omega_i^2} \tag{2}$$

Here, ω_i and ω_j are two of the eigen frequencies of the system and ξ_i and ξ_j are their corresponding damping ratios, approximately equal to 0.05. The damping ratio for each mode i can thereafter be calculated using Eq. (3).

$$\xi_i = \frac{1}{2\omega_i}\alpha + \frac{\omega_i}{2}\beta \tag{3}$$

Ground motions considered

The sufficiency of the number and type of ground motions to be considered is a matter that needs special attention in fragility analysis since a large variability is associated with ground motions. Each ground motion shows unique characteristics, leading to variability in the necessary outcomes. Current study, however, does not include uncertainty analysis and assumes a predefined value of total uncertainty factor as discussed later. The ground motions selected herein differ in their individual characteristics, such as bandwidth, dominant frequency, energy content, and strong motion duration (considered to be the time bounded by the 3% and 97% limits of the Arias Intensity) as listed in Table 2. Near-fault ground motion is usually characterized by a long-period impulsive motion in the horizontal direction, with a large amplitude both in displacement and incremental velocity. This exposes the structures to high input energy in a very short duration resulting in unexpected damage, especially in taller structures in which higher modes of vibration are also dominant [Mazza and Vulcano, 2010]. The near-fault ground motion effects are not considered in the present study.

Table 2. Characteristics of ground motions considered for time history analyses.

Sl. No.	Event	Magnitude (Mw)	Band width	Dominant frequency (rad/s)	Central frequency (rad/s)	Arias Intensity (m/s)	Strong motion duration (sec)
1	1940 Imperial Valley (El Centro)	7.1	0.94	9.20	30.00	0.16	24.02
2	1943 Indo-Burma	7.2	0.83	12.27	36.08	0.23	14.92
3	1985 Chile	7.8	0.99	11.85	41.82	0.31	33.81
4	1995 Kobe	6.9	0.88	9.12	14.75	0.13	8.56
5	1999 Kocaeli	7.6	0.94	7.17	12.86	0.22	36.83
6	1999 Duzce	7.2	0.92	18.33	37.28	0.32	12.60

Figure 5 shows the acceleration time histories of the considered ground motions on same scale. It is clear from the figure that each considered ground motion varies in terms of its modulation and total duration of strong motion. The Imperial valley (El Centro), Indo-Burma, and Duzce ground motions are similar with respect to their magnitude (Table 2), but they differ widely in their energy contents as represented by Arias Intensity which corresponds to the total energy absorbed by the frequency ensemble of un-damped SDOF systems. For a given accelerogram of total duration T_d, the energy density or accelerogram intensity ($I(t)$) is defined as the time dependent integral of acceleration (a_g) and is obtained as in Eq. (4) [Koliopoulos et al., 1998]. The maximum value of I(t) is realized at the end of the accelerogram (i.e., setting $t = T_d$).

$$I(t) = \int_0^t a_g^2(\tau)d\tau \tag{4}$$

For each ground motion, normalized energy density is plotted in Fig. 6(a) by normalizing the ground acceleration with respect to peak ground acceleration (PGA) in order to show the variation in the energy content of the ground motions. The Arias Intensity and
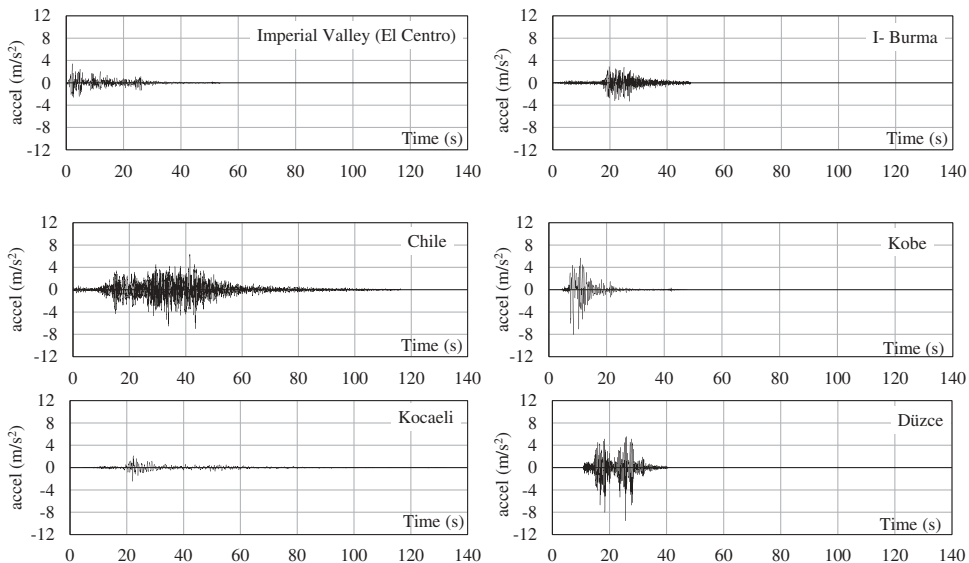
Figure 5. Acceleration time histories of the considered ground motion records.
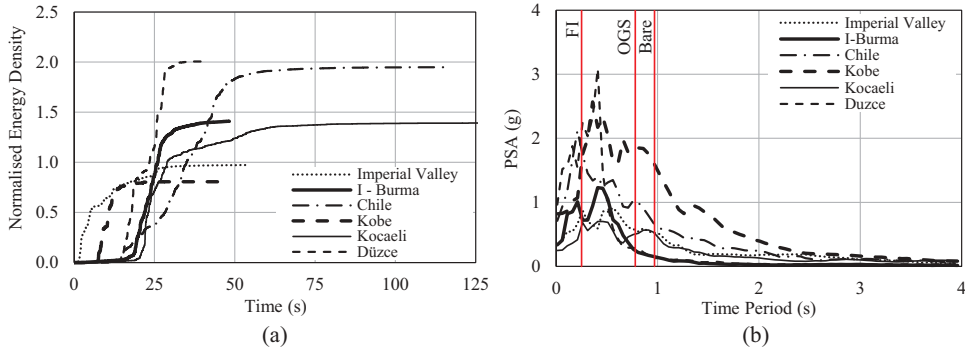
Figure 6. (a) Normalized energy density curves for the considered ground motions, and (b) Response spectrum for the considered ground motions along with the first natural period of vibration of the frames.

the energy density function are suitable measures of the damage potential of a given strong ground motion record. The large difference in the considered ground motions is also depicted by the acceleration response spectra developed for each of the considered ground motions shown in Fig. 6(b). The considered ground motions are further scaled for different PGA values within the range of 0.1 g to 1 g and used for nonlinear time history analyses of all the frames in SAP 2000.

Results of nonlinear analyses

Nonlinear static analyses

Nonlinear static analyses of the frames are first carried out in order to obtain an estimate of the capacity of the frames. The capacity is defined in terms of a lateral force-displacement curve (Fig. 7) known as pushover (PO) curve. Fig. 7 shows that the initial stiffness of the OGS frame is slightly higher than that of the BF, but the peak base shear of both the frames are quite similar. The slight change in the initial stiffness is due to the presence of infill walls as equivalent diagonal strut in the upper stories of the OGS model. In contrast, the FI frame shows very high initial
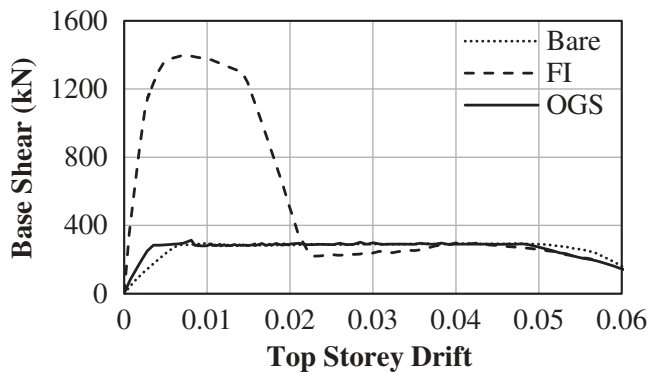

**Figure 7.** Nonlinear capacity curves for the frames.

strength and stiffness as compared to BF or OGS frame because of the presence of masonry infills in the ground story of the FI frames. Most of the lateral load is initially resisted by the ground story infills that act as compressive diagonal struts. The RC frame starts resisting the lateral loads after the masonry infill walls fail. Such lateral load sharing between the infill and the RC frame results in significant increase in lateral strength and stiffness of the FI frame in comparison to the bare or OGS frame. Although masonry infills exist in both OGS and FI frames, but the high strength and stiffness is observed in FI frames only, showing the importance of presence of infills at the ground story. In other words, the initial strength and stiffness of the frames is primarily influenced by the ground story infills; the infills in the upper stories have very less influence. At a drift of around 0.015 in the FI frame, the ground story infills fail, thus a drop in strength is observed and subsequently its strength becomes more or less similar to that of the BF or OGS frame. The presence of infill in the OGS frame has practically no influence on the strength and stiffness, and OGS frames can be treated similar to BF as far as the base shear – roof drift relation is concerned. However, the OGS frames need special attention (as discussed later) from the viewpoint of its failure, which is completely different from either BF or FI frame.

Nonlinear dynamic analyses

Nonlinear time-history analyses (NLTHA) of the frames are carried out for the selected ground motions scaled for different PGA values in the range of 0.1 g to 1 g. The resulting output are plotted in terms of story displacement and inter-story drift (ISD) demands for each ground motion at each PGA as shown in Figs. 8 and 9 for all the frames. Response of the frames in terms of each engineering demand parameter (EDP) is discussed below:
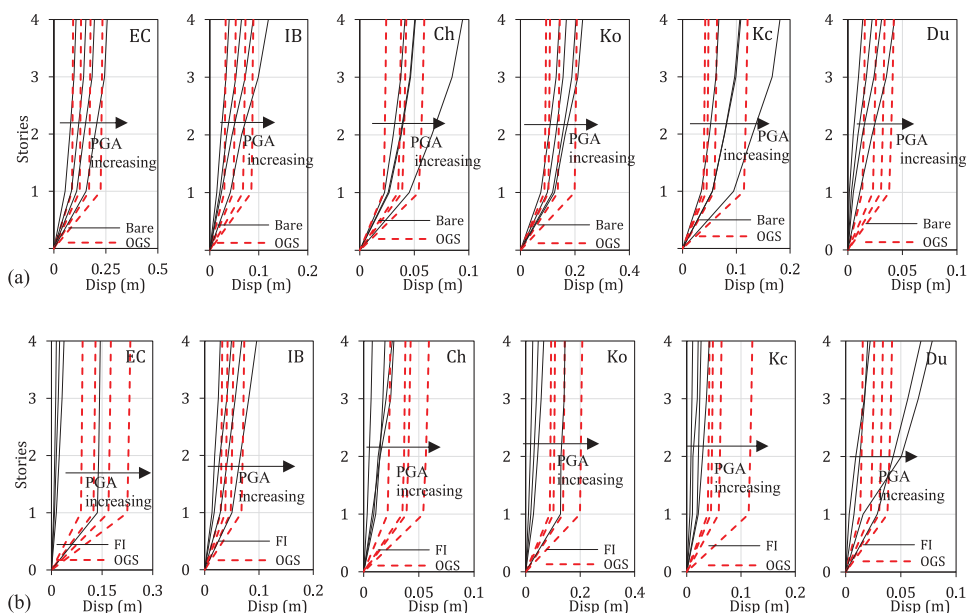
Figure 8. Peak story displacement demands for (a) Bare vs OGS frames and (b) FI vs OGS frames for El Centro (EC), I-Burma (IB), Chile (Ch), Kobe (Ko), Kocaeli (Kc) and Duzce (Du), ground motions for 0.3 g, 0.5 g, 0.7 g and 1 g.
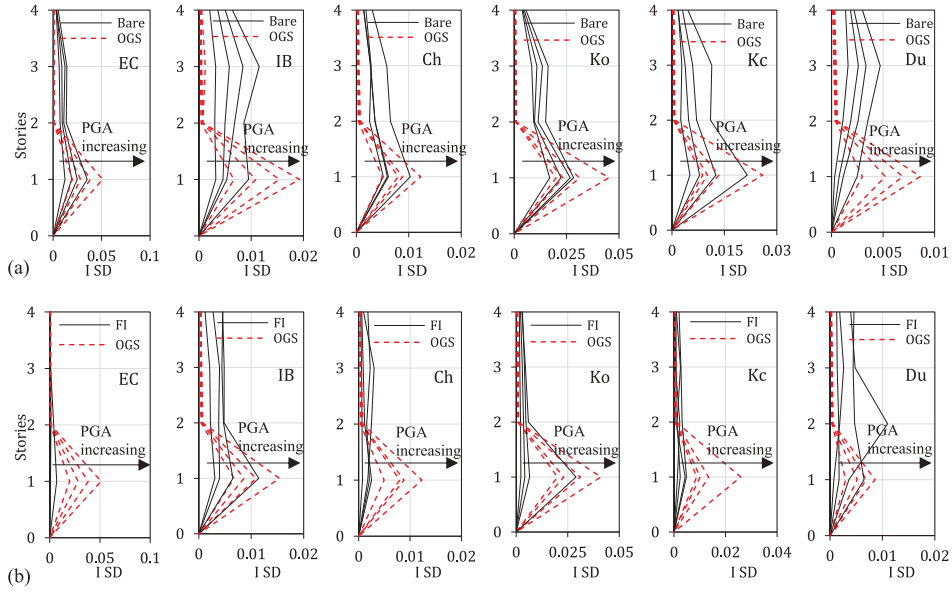
Figure 9. Peak ISD demands for (a) bare vs OGS frames and (b) FI vs OGS frames for El Centro (EC), I-Burma (IB), Chile (Ch), Kobe (Ko), Kocaeli (Kc) and Duzce (Du), ground motions for 0.3 g, 0.5 g, 0.7 g and 1 g.

(i) Considering maximum story displacement as the EDP

First the maximum story displacement is considered as the engineering demand parameter in NLTHA, and the peak story displacement demands of the OGS frames are compared with that of the bare frames in Fig. 8(a) for the ground motions considered at different PGA levels. In most ground motions and at any PGA, the top level (TL) peak displacement of BFs is equal to or greater than of the OGS frames. The story displacement decreases from top to bottom stories in BF. However, in OGS frames, the peak displacement is achieved at the ground story level (GL) itself and it is maintained in the upper stories. The difference in the peak displacement of BFs and OGS frames increases with increasing PGA. At ground story, the OGS frames show higher displacement demand as compared to the bare frame. Since most of the lateral deformation in the OGS frames is concentrated in the ground story level and there is insignificant relative deformation in the upper stories, the top displacement may not be the critical displacement to be considered in fragility assessment of OGS frames.

Figure 8(b) shows the comparison of deformation behavior of OGS frames with FI frames in terms of peak story displacement. The FI frames deform gradually from bottom to top level. However, unlike BFs, the FI frames show a displacement pattern similar to that of OGS frames for some ground motions with higher PGA. This happens due to early failure of the ground story infills, after which the FI frames show irregular frame deformation pattern. Thus, considering peak story displacement at top story as EDP, it is difficult to recognize the location of failure in OGS as well as in the FI frames.

(ii) Considering maximum inter-story drift (ISD) as EDP

As an alternative to considering peak story displacement as EDP, maximum inter-story drift (ISD) is considered as EDP in the next set of NLTHA. Figure 9 shows the story-wise peak inter-story drift (ISD) profile of BFs, OGS frames, and FI frames obtained for the considered ground motions. The ISDs are computed as the difference of peak displacements between the adjacent stories normalized with respect to height of the story considered. Figure 9(a) shows that for any PGA, the OGS frames undergo a very high ISD demand in ground story compared to any other story. Subsequently, a sudden reduction of ISD is evident from ground story to upper stories in OGS frames. The ISD demand in the upper stories of OGS frames is almost nil, implying that there is no relative displacement in the upper stories. This happens because the infills present in the upper stories make the upper stories stiff in comparison to the ground story, which is open. The whole upper stories, thus, move as a solid rigid mass with little or no relative deformation in between the stories. Therefore, the relatively flexible ground story columns are subjected to high ductility demand for which they are not generally designed. This leads to heavy damage in OGS columns, and hence, catastrophic failure of the OGS frames. In contrast, the BFs mostly show a uniform ISD demand along the height as compared to OGS frames, indicating that the lateral forces are resisted uniformly by columns of all the floors. Figure 9(b) shows that the ISD demands for FI frames are very less as compared to the OGS frames. Further, the FI frames also show more or less a uniform distribution of drift demands along the height of the frames. At higher PGA, however, some ground motions cause very high drift demands in the ground story columns of the FI frames. Lateral behavior of FI frames for such ground motions is quite similar to OGS frames. As already discussed, this is basically the outcome of failure of ground story infills at higher PGA.

Overall, it is observed that the regular frames (BFs and FI frames) deform uniformly along the height of the building. However, for some ground motions in FI frames, the ground story infills fail early leading to formation of a frame system similar to an OGS frame. Thus, the deformation behavior of the FI frames (after failure of infills) becomes similar to that of an OGS frame showing highest displacement at the ground story and almost same and constant displacement at all upper floors. This shows that the global displacement of the frame is inadequate in predicting the local effect that takes place in the ground story columns of both FI and OGS frames. The story level performance or the local behavior is required to be well captured through the use of component level demand parameter, (e.g., GL-ISD) in order to estimate the fragility satisfactorily. Thus, the choice of EDP for prediction of damage and localized failure pattern in irregular frames and in those regular frames, which may become irregular during seismic excitation must be emphasized.

It is clear from Figs 8 and 9 that the local level or component level demand parameter is more efficient in portraying the realistic response of irregular frames. Therefore, in Figs 10 and 11, only the displacement and ISD demands at GL and TL are compared for all the frames under different ground motions with varying PGA values. Fig. 10 clearly shows that the peak lateral displacement of BFs is consistently more at TL for all earthquakes with all PGAs. Similarly, in case of FI frames, though the TL displacement is more than the GL displacement, the difference is not uniform and consistent as observed in BFs. As already discussed, this is because of the early
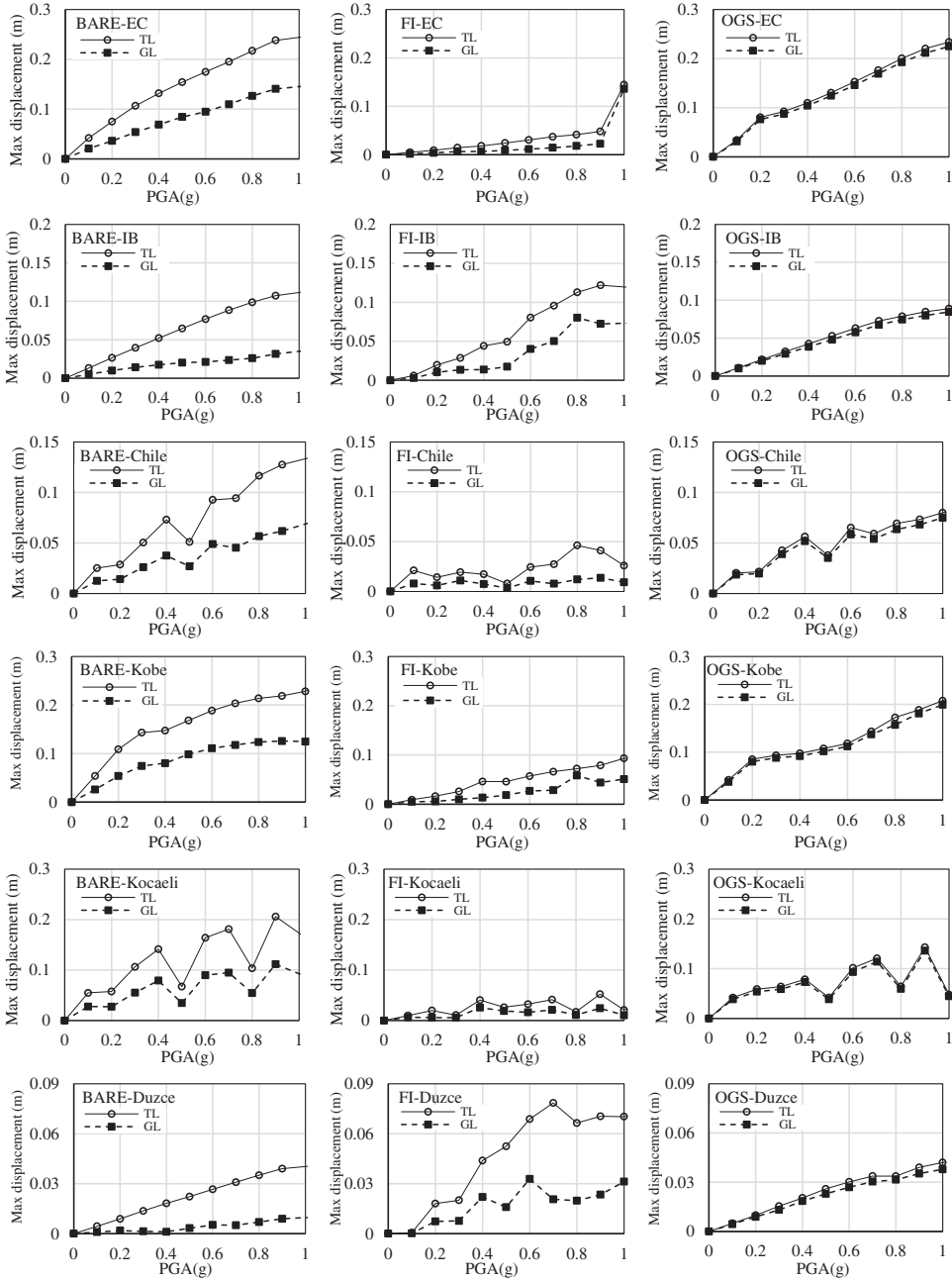
Figure 10. Variation of maximum displacement at top level (TL) and ground story level (GL) for BF, FI frame and OGS frame for different ground motions.

brittle failure of masonry infill walls in ground story of FI frames under some ground motions. Contrastingly, there is practically no difference in the peak displacement at TL and GL in case of OGS frames for all the ground motions.
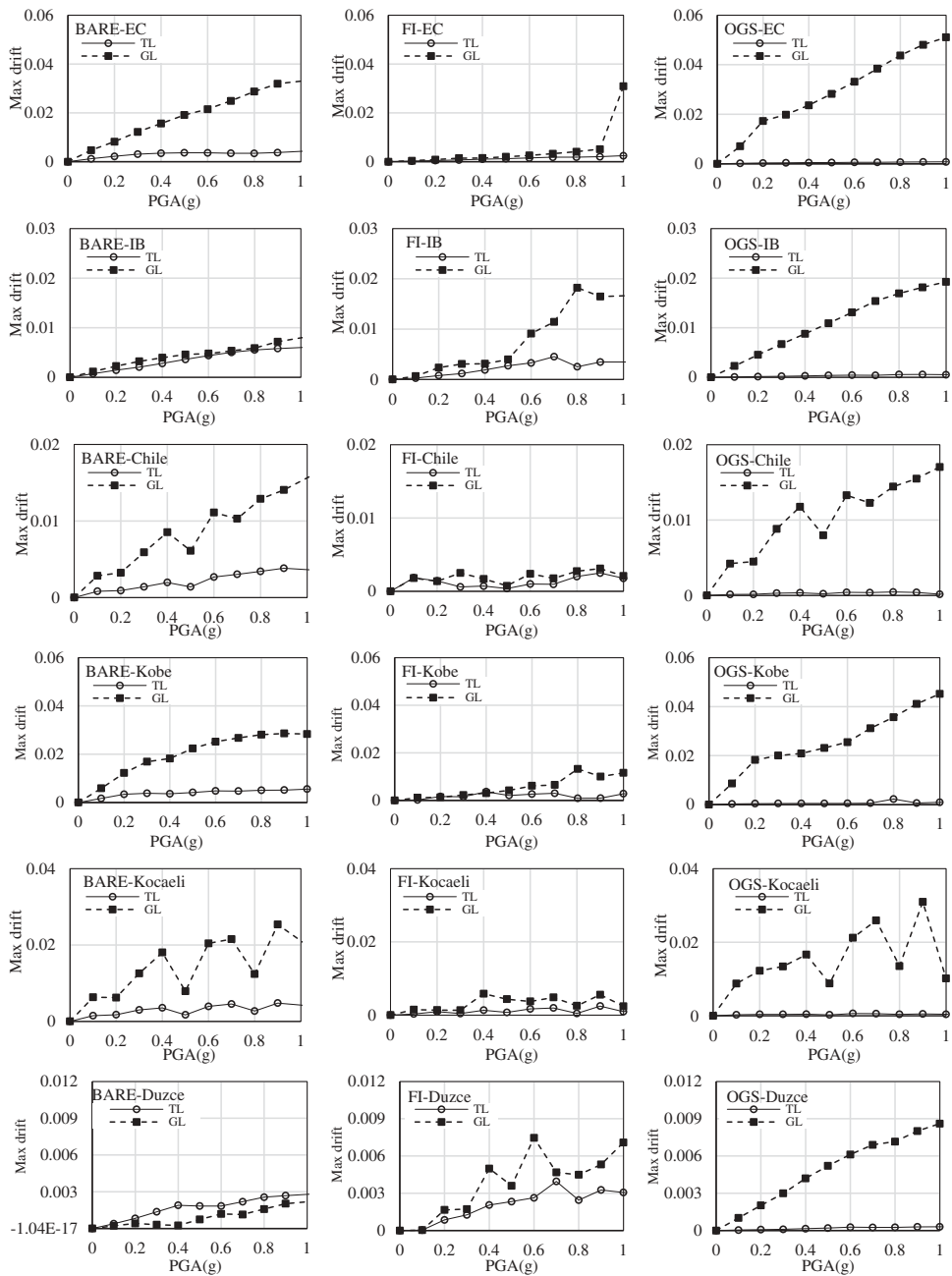
Figure 11. Variation of maximum inter-story drift at top level (TL) and ground level (GL) for BF, FI frame and OGS frame for different ground motions.

This clearly shows that the TL displacement can be conveniently taken as EDP for BFs and to certain extent for FI frames, since TL displacement is the critical displacement. But it is difficult to form such an opinion for OGS frame since both TL and GL show almost equal displacement and both the displacements appears to be critical. To look into the component level behavior,

ISD at each story is plotted for TL and GL only as shown in Fig. 11. Interestingly, the deformation behavior of OGS frames changes completely on plotting the ISD demand; a very high GL-ISD demand is observed as compared to the TL-ISD. However, this difference is not much in case of FI frame or BF. The TL-ISD in case of OGS frame is nearly zero. This proves that the ground story columns are subjected to high ISD demand. In other words, there occurs a huge rotation in the columns of the ground story of OGS frames, whereas, there is no rotation in all the upper story columns. As discussed already, this is obvious due to the absence of infill in the ground story of OGS frames. Clearly, the ground level columns are much more susceptible to damage compared to the top floor columns. This behavior is similar to the actual damage and failure observed in OGS buildings during past earthquakes, where huge rotation, and hence, damage was observed to be concentrated in the ground story columns with a little relative deformation in the upper stories. This failure pattern of OGS frames is well captured analytically by considering the ISD at ground story as EDP.

Therefore, from Fig. 11 it is clear that the GL-ISD in OGS frames, for all ground motions with all PGAs, represent a better and realistic EDP for damage or fragility assessment. On the other hand, the peak lateral ISD at GL and TL for bare frames and FI frames (i.e., mostly regular frames) do not show a consistent variation across ground motions. For most of the ground motions considered, the peak ISD at the TL and GL are nearly identical in case of FI frames, except at higher PGA, where the GL drift is higher as compared to roof drift. Therefore, peak lateral displacement at top story may be used as EDP for damage or fragility assessment of regular frames. In case of BF, it is observed that for some cases of ground motion, GL-ISD is more critical than TL-ISD, similar to OGS frames. However, the value of ISD-TL of BF is higher compared to TL-ISD of OGS frame, which is negligible. Thus, choice of a suitable EDP representing the true behavior or failure pattern is of concern particularly in case of irregular frames.

Figure 12 represents the median of the frame responses obtained from NLTHA for all ground motions. The maximum displacement at the top level or maximum drift over the height of the building (i.e., total drift at TL) are the two most commonly used EDPs for seismic performance assessment. For such EDPs, the BFs show maximum response (Fig. 12(b)) compared to FI or OGS frames. Similarly, when ISD at TL (Fig. 12(d)) is considered as EDP, the BF again shows highest response for a given PGA. Contrastingly, when displacement or ISD at GL (Figs 12(a) and (c)) is considered as EDP, the OGS frames show the highest response. With respect to ISD-TL as the EDP, the OGS frames show the least response which is in contrasting to TL-ISD as EDP that shows the highest response. The displacement at GL or the GL-ISD shows highest response for OGS frame which is realistic and relates well to the past earthquake damage.

Seismic damage assessment and fragility analysis

Seismic damage and fragility assessment is the numerical quantification of probable damage to a building caused due to a given hazard. In order to physically categorize the degree of damage to the members of a building under an earthquake of a specific intensity, damage states are specified. The damage states and fragility estimation based on these damage states for different EDPs are discussed in this section.
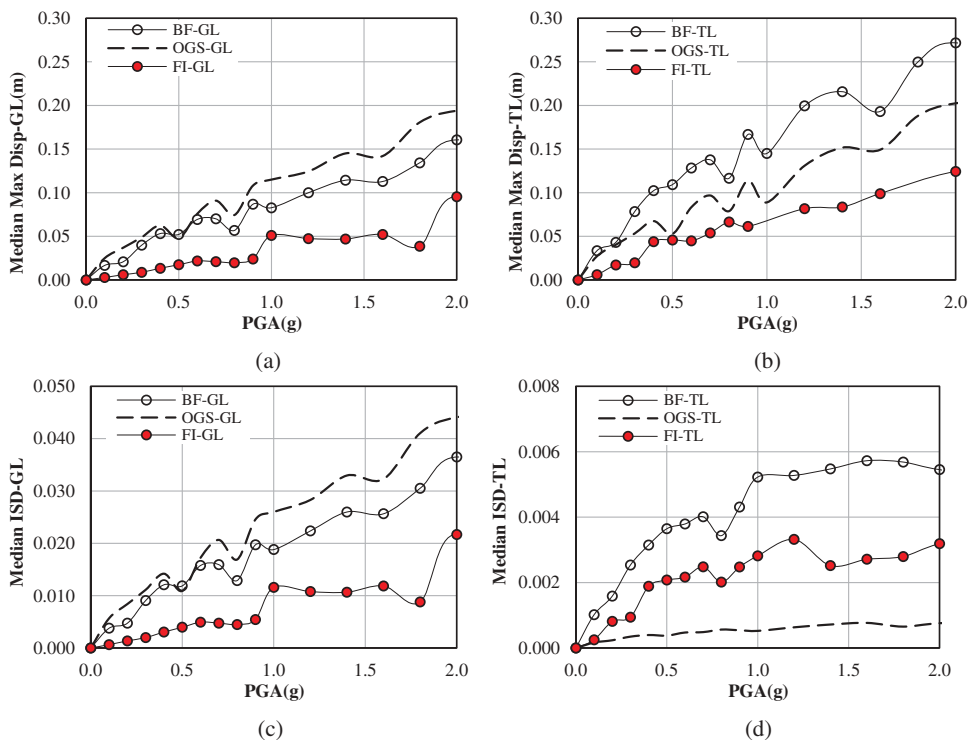
Figure 12. Median response at GL and TL obtained for BF, OGS frame and FI frame for all the ground motions.

Description of damage states

Several damage indices are proposed in the past literature to numerically interpret thresholds for damage states in terms of strength or parameters related to ductility and hysteretic energy dissipation. Such relationships are available in the literature [e.g., Lagomarsino and Giovinazzi, 2006; Barbat et al., 2008] for different frame configurations, where the damage states are expressed in terms of capacity curve parameters, for example, yield displacement and ultimate displacement. Other parameters, such as maximum base shear capacity [Silva et al., 2014] or inter-story drift ratio [HAZUS, 2013] have also been used in the past to quantify the damage. The damage states specified in HAZUS [2013] for mid-rise RC buildings are used in the present study; slight (S), moderate (M), extreme (E), and complete (C) are the four damage states for which the average inter-story drift thresholds (Δ_{ds}) are specified in HAZUS (Table 3). The frames considered are categorized under two

Table 3. Average inter-story drift thresholds (Δ_{ds}) as specified in HAZUS (2013).

	Δ_{ds}	
Damage States	C1	C3
Slight (S)	0.0033	0.002
Moderate (M)	0.0053	0.004
Extreme (E)	0.0130	0.010
Complete (C)	0.0330	0.023

different model building types of HAZUS: the BFs are classified as C1-M frames and both FI and OGS frames are classified as C3-M type frames designed for low code seismic level.

Seismic fragility assessment

The most common form of seismic fragility function is the lognormal cumulative distribution function and is of the form given in Eq. (5). $P[x \geq \theta_d|IM]$ represents the conditional probability of exceedance of the EDP (here, x) with respect to θ_d, given intensity measure (IM), such as PGA. Φ represents the standard normal probability, θ_d is the median value of EDP, that is, inter-story drift, considered as per HAZUS [2013] for different damage states considered. The drift thresholds are suitably converted to displacement thresholds to estimate the seismic fragility in terms of displacement. Estimation of uncertainty is an important step in fragility analysis. The total uncertainty in fragility estimation (β_d) is considered to be 0.7 [Kaushik and Choudhury, 2015] as summation of uncertainty in modeling, ground motions, and damage state medians.

$$P[\text{x} \geq \theta_\text{d}|\text{IM}] = \Phi\left(\frac{\ln(\text{x}/\theta_\text{d})}{\beta_\text{d}}\right) \qquad (5)$$

The seismic fragilities for all the frames are estimated for six ground motions by varying PGA from 0.1 g to 1.0 g using Eq. (5) considering the following EDPs at various floor levels:

i. Peak Top level (TL) or Peak roof displacement as EDP

Figure 13 shows the seismic fragility of BF, OGS, and FI frames for two PGA (0.5 g and 0.7 g) evaluated considering peak roof or top level (TL) displacement as EDP obtained from the nonlinear time history analyses. Discrete seismic fragilities are obtained for each of the ground motions at the considered four damage states (S, M, E, and C). Figure 13(a) shows the comparison of discrete fragilities of OGS frames with those of BFs for the two PGA levels only. Similarly, Fig. 13(b) shows the comparison of discrete fragilities obtained for OGS frames with FI frames.

Figure 13(a) shows that for both PGA (0.5 g, 0.7 g), BFs are less fragile than OGS frames for slight damage state, whereas, for higher damage states (M, E, C), the fragility of the two frames (BF and OGS) do not change uniformly. Similarly, Fig. 13(b) shows that for 0.5 g PGA, the FI frames are less fragile than OGS frames for any damage state. But with increasing PGA, the difference in fragility of FI and OGS frames is not uniform. Similar trend of fragility variation was observed for other PGAs as well (0.1 g to 1.0 g).

Thus, when the TL displacement is considered as an EDP, no definite fragility pattern can be established as observed from the comparison of OGS frames with either BFs or FI frames. Experience from past earthquakes certainly hints toward higher seismic fragility of OGS frames because of their poor performance compared to BFs or FI frames. However, the fragility estimation with roof displacement as an EDP gives a wrong essence of the physical behavior or failure pattern of irregular OGS frames under the effect of seismic input. Some cases show early failure of the bare or FI frames compared to OGS frames, for a given PGA. Whereas, in some other cases, OGS frames fail early compared to the regular frames (either bare or FI frames). In many cases, OGS frames are seen to be less fragile and hence less vulnerable as compared to either BF or FI frames. Such results are
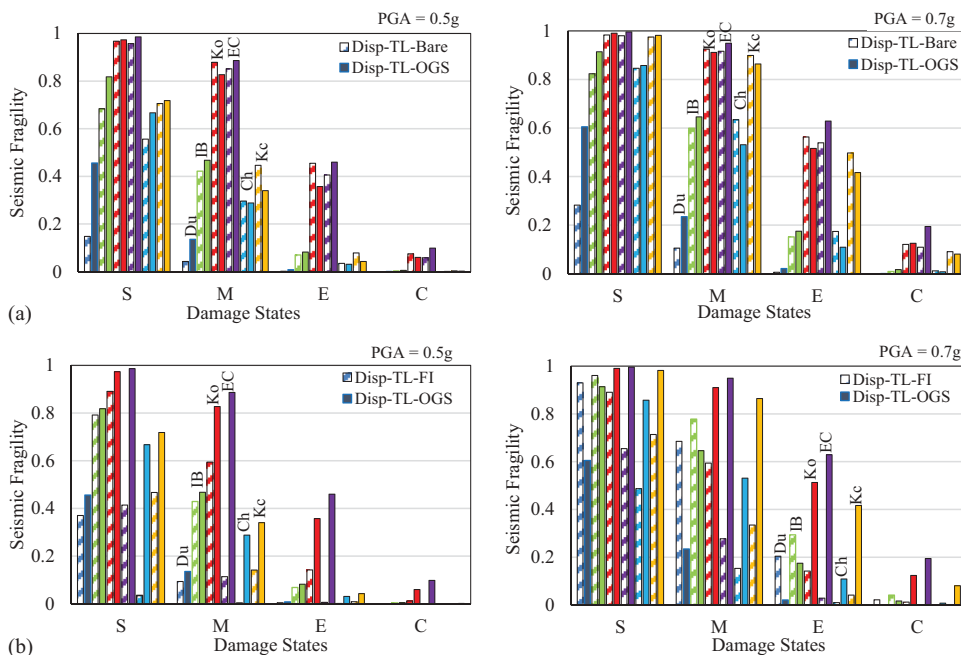
Figure 13. Comparison of seismic fragility obtained for two PGA levels considering top level displacement as EDP: (a) BFs vs OGS frames (b) FI frames vs OGS frames.

contradictory to the past experiences from earthquake, where the OGS buildings are found to have failed even during minor shaking. Thus, this choice of EDP needs to be revised and modified for irregular frames, such as OGS frames.

ii. Story displacement corresponding to Peak TL displacement as EDP

Seismic fragility with respect to displacement at all the floors corresponding to peak displacement at roof or top level is obtained by considering linear distribution of the threshold displacements along the building height. The average inter-story drift (Δ_{ds}) threshold is multiplied by the respective height of each floor of the building to obtain the displacement threshold as per HAZUS [2013].

14(a) and (b) show comparative discretefragility of BFs vs OGS frames and FI vs OGS frames, respectively, estimated considering story displacement corresponding to peak displacement at roof or top level of the building frames as the EDP. The displacement at the other floors is obtained at the time instant when the displacement at top level is maximum. The figures represent seismic fragility values obtained for El Centro ground motion for different PGA values at all damage states. On observing from top to bottom story of each building frame, the seismic fragility at the ground story of OGS frame is observed to be the highest. Also, the fragility of OGS frame is higher than that of the BF as well as FI frames at ground story for any ground motion and any PGA value.

The OGS frames are most fragile at the ground story as observed during past earthquakes. The open ground story being flexible undergoes highest relative deformation compared to upper stories, and hence damage is concentrated only at the columns of
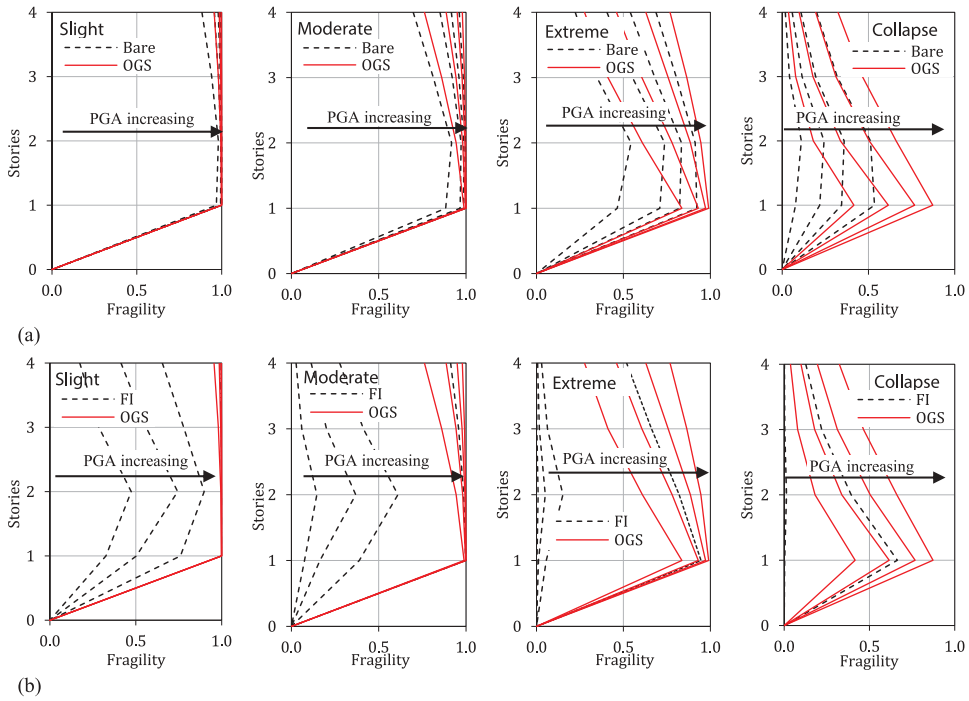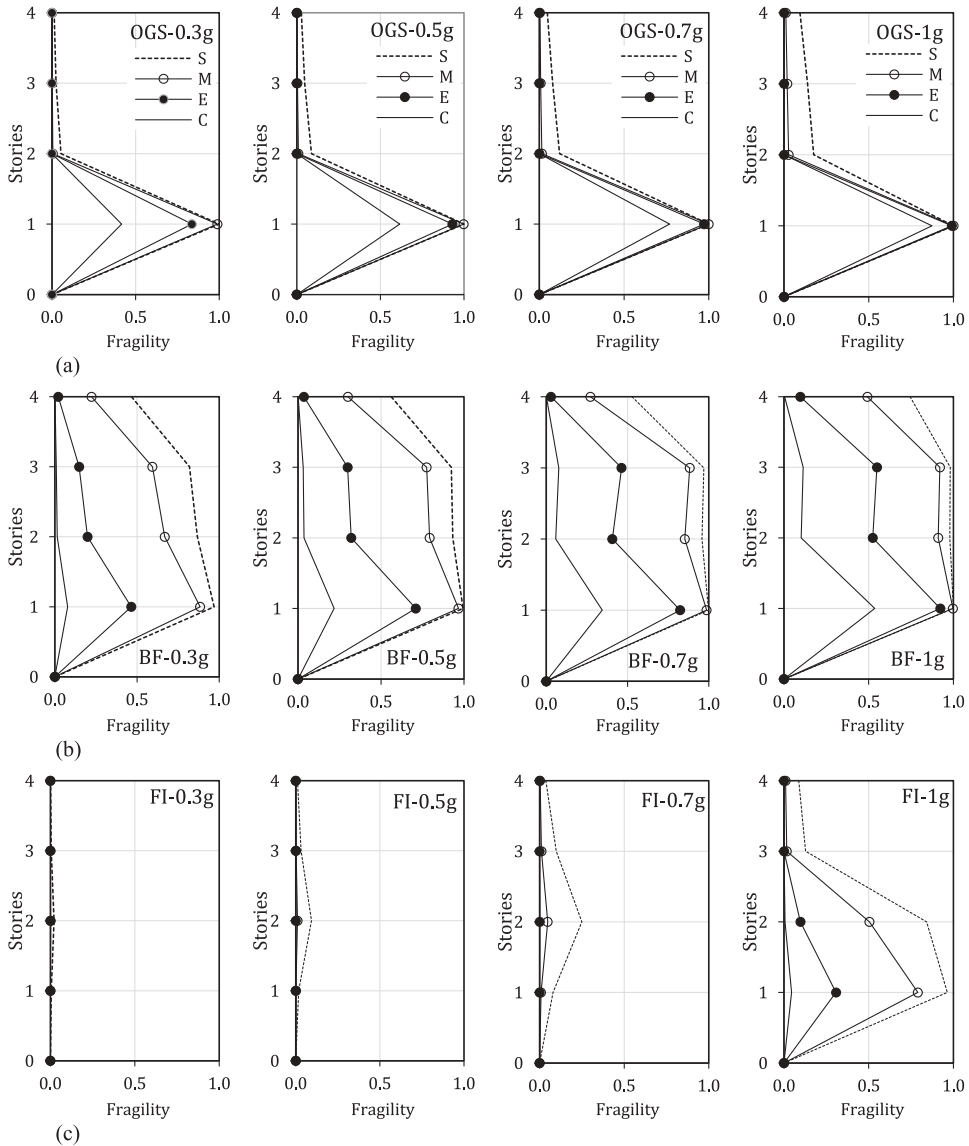
Figure 14. Story wise fragility profile considering displacement demand at each floor level obtained from time history analysis for El Centro ground motion scaled for different PGA (0.3 g, 0.5 g, 0.7 g, 1 g): (a) BF vs OGS frame, (b) FI frame vs OGS frame.

ground story without any damage to the upper story columns. This type of damage distribution along the height is, however, not reflected in the fragility estimated using the story displacement at each floor level corresponding to peak TL displacement as an EDP. It is clear from Fig. 14(a) that though the fragility of the upper floors of OGS frames is lesser than that of the adjacent lower floors in each frame, the upper story columns are also fragile and undergo significant damage. Therefore, although this is the most common choice for EDP to estimate fragility for regular frames, it does not give the true essence of the fragility for the irregular frames. Similarly, the fragilities of BFs and FI frames are quite high at the second floor level, which also does not reflect the realistic damage observed in such frames during past earthquakes.

iii. Inter-story drift (ISD) at each floor level as EDP

Fragility with respect to peak ISD at each story is obtained by considering the drift thresholds for each damage state as suggested in HAZUS [2013]. As expected, the seismic fragility of OGS frames is almost nil in upper stories, whereas, it is maximum at the ground story level (Fig. 15a), which resembles observed damage in real buildings, since the OGS frame fails due to the failure of the open ground story columns. In contrast, the fragility of bare frames (Fig. 15b) is distributed throughout the height of the building obviously with highest fragility at the ground story level. The OGS columns are found to be more vulnerable than the bare frame ground story columns, which is obvious. Hence,

Figure 15. Story wise fragility profile of the frames considering ISD demand at each floor obtained from time history analysis for El Centro ground motion scaled for different PGA (0.3 g, 0.5 g, 0.7 g, 1 g): (a) OGS frames, (b) Bare frames, (c) FI frames.

this form of representation of EDP can give us a better estimation and understanding of the fragility in terms of damage incurred in irregular frames, such as OGS frames. Fragility obtained with respect to ISD as EDP clearly differentiates the failure pattern of the regular and irregular frames.

Figure 15(c) shows the discrete fragilities obtained for FI frames for the four damage states at different PGA levels. The FI frame shows higher fragility at the upper floors at each damage state for lower PGA (upto about 0.7 g), after which, the ground story becomes more fragile as seen at a PGA of 1 g. As already discussed, this happens due to

the failure of ground story infills at higher intensities of ground motion. For lower intensities of ground motion (i.e., from 0.1 g to 0.7 g PGA), it is observed that the FI frame shows fragility pattern similar to the BF. This suggests that for lower intensity ground motions, the ground story infills resist most of the lateral load without early failure, and therefore, the FI frames behave like a regular frame, and undergo damage throughout the height of the building. As soon as the ground story infills fail with increasing intensity of ground motion, a soft story is created in the FI frames at the ground story, and hence it starts behaving like an OGS frame.

Figure 16 further supports these observations, where it can be clearly seen that the seismic fragility of the top story columns of the OGS frames, obtained using peak ISD at top story as EDP, is almost nil compared to those of either BFs (Fig. 16a) or FI frames (Fig. 16b). Figure 16 is plotted for all ground motions with PGA of only 0.5 g, however, the results are equally applicable to all PGA levels considered in the study.

iv. Inter-story drift at ground story level as EDP

Figure 17 shows the component level fragility obtained for the ground story columns computed considering the peak inter-story drift (ISD) demand at GL as EDP for BFs, OGS frames, and FI frames for PGA of 0.5 g. Clearly, from the comparison of the fragility values of the frames, the ground story columns of OGS frames are found to be consistently
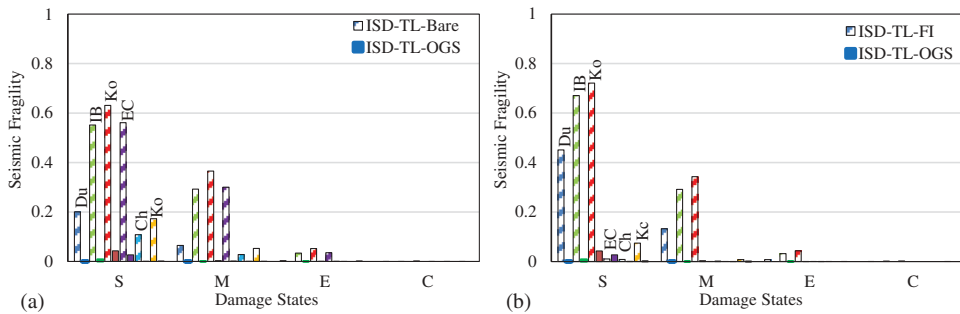
Figure 16. Seismic fragility of columns of the top story considering top level ISD as EDP for PGA of 0.5 g: (a) Bare frame vs OGS frame and (b) FI vs OGS frame.
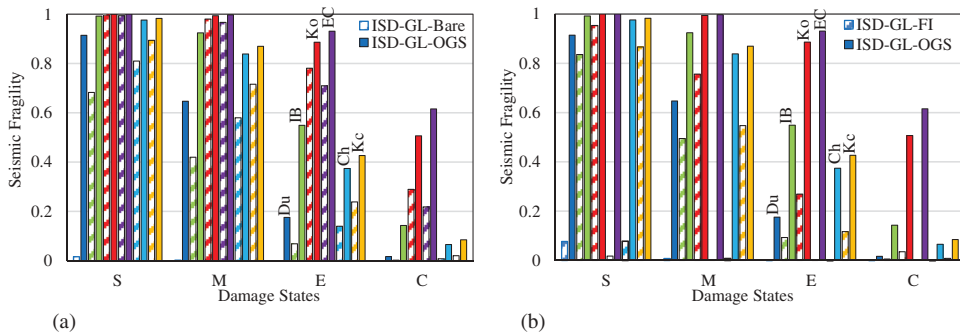
Figure 17. Seismic fragility of ground story columns of frames considering ground story level ISD as EDP for PGA of 0.5 g: (a) Bare frame vs OGS frame and (b) FI vs OGS frame.

more fragile than those of BF (Fig. 17a) or FI frame (Fig. 17b) even for low damage states. Similar results are obtained for other PGA values as well.

It can be stated that the choice of EDP for fragility estimation should depend on buildings' physical behavior. Seismic fragility of regular RC moment frames, such as the bare frames, can be estimated easily considering top displacement as the EDP, since in such buildings the displacement at the top or roof is critical and it decreases uniformly as we go down to the bottom storys. Whereas, consideration of EDP for RC moment frames with masonry infill walls depends on the existence of the irregularity (a soft or flexible story) in the building frame. For the typical case of OGS frame as an irregular frame, it is found that the ground story columns are more vulnerable than the upper story columns. OGS frame have localized damage mainly at the level where the irregularity lies, that is, at the ground story columns, with negligible or no damage in the upper floors. Fragility description at component level helps in locating the members that can be actually damaged and need repair or retrofitting. Instead of considering global roof or top level displacement, when local demand parameters, such as ISD at each story are considered, the localized fragility of the members in consideration can be realistically estimated at a component level.

Conclusion

Seismic fragility of three common typologies of concrete moment frames, broadly categorized as frame with unreinforced masonry infill walls and those without infill walls are studied. Different configuration of masonry infill walls in the frame may sometimes render the frame highly irregular, for example, open ground story frames in which masonry infill walls are not provided in the ground story. Experience during past earthquakes suggests that the open ground story buildings behave poorly during earthquake shaking. Such buildings suffered severe damage in the ground story columns but no noticeable damage was observed in the upper stories. It is observed in the nonlinear time history analyses of the considered frames for six ground motions that the conventional engineering demand parameters (EDP), for example, top level displacement or drift, cannot capture this behavior of open ground story frames, and hence, the fragility estimated using such EDP will not be realistic.

The primary objective of the study is to establish an EDP that correctly interprets the behavior of irregular frames for fragility assessment. This is accomplished by considering both displacement and inter-story drift as engineering demand parameters for fragility assessment of regular and irregular frames. Equal importance is laid on the effect of infills and its presence or absence in the ground story of the frames. It is obviously observed in the fragility estimation that the absence of infills in the ground story makes the frame more vulnerable as compared to a frame without any infill in any story (bare frame). Further, a frame with infill walls in all the stories becomes vulnerable once the ground story infills fail, which otherwise, behaves as a regular frame.

To understand and clearly bring the outcome of physical behavior of irregular frames into analytical results, it is shown and suggested in the study that a component level demand parameter (such as inter-story drift) must be considered at the level of irregularity for realistic fragility assessment of irregular frames. For example, for open ground story frames, the inter-story drift of the ground story gives better representation of building's

lateral performance, and therefore, must be preferred as EDP for fragility estimation. Consideration of roof displacement as EDP (conventional method) does not suffice the contemporary need for seismic analysis of irregular frame behaviors. Further, it is also observed that using the conventional EDP (roof displacement or lateral drift at top level) is quite simple and effective for fragility assessment of regular frames.

Based on the nonlinear time history analysis of the three frames considered, this study draws conclusion on the behavioral aspect of the frames. Comparative displacement response as well as fragilities is obtained for the frames considering different EDPs. Although each of the ground motion leads to the same conclusion, more number of ground motions should be considered for any firm conclusion to be drawn. Further, it is to be mentioned that only in-plane behavior of the frames is considered in the present study. The study is carried out considering only one building geometry. Though the behavior of buildings with different geometry will be different, the conclusions drawn in the present study are general in nature and can be applied to buildings with different geometries.

Funding

References

Aschheim, M., Gülkan, P., Sezen, H., Bruneau, M., Elnashai, A., Halling, M., Love, J. and Rahnama, M. [2000] "Performance of buildings," *Earthquake Spectra, EERI* **16**(S1), 237–279. doi:10.1193/1.1586155.

Bai, J. W., Gardoni, P. and Hueste, M. B. D. [2011] "Story-specific demand models and seismic fragility estimates for multi-story buildings," *Structural Safety* **33**(1), 96–107. doi:10.1016/j.strusafe.2010.09.002.

Barbat, A. H., Pujades, L. G. and Lantada, N. [2008] "Seismic damage evaluation in urban areas using the capacity spectrum method: Application to Barcelona," *Soil Dynamics and Earthquake Engineering* **28**(10), 851–865. doi:10.1016/j.soildyn.2007.10.006.

BIS. [2002] *Indian Standard 1893 (Part 1), Criteria for Earthquake Resistant Design of Structures: Part 1 General Provisions and Buildings*, 5th Rev., Bureau of Indian Standards, New Delhi, India.

Cavaleri, L. and Di Trapani, F. [2014] "Cyclic response of masonry infilled RC frames: Experimental results and simplified modeling," *Soil Dynamics and Earthquake Engineering* **65**, 224–242. doi:10.1016/j.soildyn.2014.06.016.

Choudhury, T. and Kaushik, H. B. [2018] "Seismic fragility of open ground story RC frames with wall openings for vulnerability assessment," *Engineering Structures* **155**, 345–357. doi:10.1016/j.engstruct.2017.11.023.

CSI. [2015] *Structural Analysis Program, SAP2000– Advanced, Static and Dynamic Finite Element Analysis of Structures*, Computers and Structures Inc. (CSI), Berkeley, USA.

Dolšek, M. and Fajfar, P. [2001] "Soft story effects in uniformly infilled reinforced concrete frames," *Journal of Earthquake Engineering* **5**(1), 1–12. doi:10.1080/13632460109350383.

Ellingwood, B. R., Celik, O. C. and Kinali, K. [2007] "Fragility assessment of building structural systems in Mid-America," *Earthquake Engineering & Structural Dynamics* **36**(13), 1935–1952. doi:10.1002/(ISSN)1096-9845.

FEMA. [2000] *Prestandard and Commentary for the Seismic Rehabilitation of Buildings, FEMA 356*, Federal Emergency Management Agency, Washington, DC.

Freddi, F., Padgett, J. E. and Dall'Asta, A. [2017] "Probabilistic seismic demand modeling of local level response parameters of an RC frame," *Bulletin of Earthquake Engineering* **15**(1), 1–23. doi:10.1007/s10518-016-9948-x.

Hahn, G. T., Bhargava, V. and Chen, Q. [1990] "The cyclic stress-strain properties, hysteresis loop shape, and kinematic hardening of two high-strength bearing steels," *Metallurgical Transactions A* **21**(2), 653–665. doi:10.1007/BF02671936.

HAZUS. [2013] *HAZUS - MH MR5, Advanced Engineering Building Module (AEBM), Technical and User's Manual*, FEMA, Washington, D.C.

Jalayer, F. and Cornell, C. A. [2009] "Alternative non-linear demand estimation methods for probability-based seismic assessments," *Earthquake Engineering & Structural Dynamics* **38**(8), 951–972. doi:10.1002/eqe.v38:8.

Kaushik, H. B. and Choudhury, T. [2015] "Vulnerability analysis of buildings for seismic risk assessment: A review," *The Bridge and Structural. Engineer, the Journal Of. Indian National Group (ING) of International Association for Bridge and Structural. Engineering. (IABSE)* **45**(1), 63–76.

Kaushik, H. B. and Jain, S. K. [2007] "Impact of great December 26, 2004 Sumatra earthquake and tsunami on structures in Port Blair," *Journal of Performance of Constructed Facilities* **21**(2), 128–142. doi:10.1061/(ASCE)0887-3828(2007)21:2(128).

Kaushik, H. B., Rai, D. C. and Jain, S. K. [2007, September] "Stress-strain characteristics of clay brick masonry under uniaxial compression," *Journal of Materials in Civil Engineering* **19**(9), ASCE, 728–739. doi:10.1061/(ASCE)0899-1561(2007)19:9(728).

Kaushik, H. B., Rai, D. C. and Jain, S. K. [2009] "Effectiveness of some strengthening options for masonry-infilled RC frames with open first story," *Journal of Structural Engineering, ASCE* **135**(8), 925–937. doi:10.1061/(ASCE)0733-9445(2009)135:8(925).

Kazantzi, A. K. and Vamvatsikos, D. [2015] "Intensity measure selection for vulnerability studies of building classes," *Earthquake Engineering & Structural Dynamics* **44**(15), 2677–2694. doi:10.1002/eqe.v44.15.

Koliopoulos, P. K., Margaris, B. N. and Klimis, N. S. [1998] "Duration and energy characteristics of Greek strong motion records," *Journal of Earthquake Engineering* **2**(3), 391–417. doi:10.1080/13632469809350328.

Lagomarsino, S. and Giovinazzi, S. [2006] "Macroseismic and mechanical models for the vulnerability and damage assessment of current buildings," *Bulletin of Earthquake Engineering* **4**(4), 415–443. doi:10.1007/s10518-006-9024-z.

Liu, X. X., Wu, Z.-Y. and Liang, F. [2016] "Multidimensional performance limit state for probabilistic seismic demand analysis," *Bulletin of Earthquake Engineering* **14**(12), 3389–3408. doi:10.1007/s10518-016-0013-6.

Mander, J. B., Priestley, M. J. and Park, R. [1988] "Theoretical stress-strain model for confined concrete," *Journal of Structural Engineering, ASCE* **114**(8), 1804–1826. doi:10.1061/(ASCE)0733-9445(1988)114:8(1804).

Mazza, F. and Vulcano, A. [2010] "Nonlinear dynamic response of RC framed structures subjected to near-fault ground motions," *Bulletin of Earthquake Engineering* **8**(6), 1331–1350. doi:10.1007/s10518-010-9180-z.

Mondal, G. and Tesfamariam, S. [2014] "Effects of vertical irregularity and thickness of unreinforced masonry infill on the robustness of RC framed buildings," *Earthquake Engineering & Structural Dynamics* **43**(2), 205–223. doi:10.1002/eqe.v43.2.

Ramamoorthy, S. K., Gardoni, P. and Bracci, J. M. [2006] "Probabilistic demand models and fragility curves for reinforced concrete frames," *Journal of Structural Engineering* **132**(10), 1563–1572. doi:10.1061/(ASCE)0733-9445(2006)132:10(1563).

Ruiz-García, J. and Miranda, E. [2006] "Evaluation of residual drift demands in regular multi-story frames for performance-based seismic assessment," *Earthquake Engineering & Structural Dynamics* **35**(13), 1609–1629. doi:10.1002/(ISSN)1096-9845.

Ruiz-García, J. and Miranda, E. [2010] "Probabilistic estimation of residual drift demands for seismic assessment of multi-story framed buildings," *Engineering Structures* **32**(1), 11–20. doi:10.1016/j.engstruct.2009.08.010.

Silva, V., Crowley, H., Varum, H., Pinho, R. and Sousa, R. [2014] "Evaluation of analytical methodologies used to derive vulnerability functions," *Earthquake Engineering & Structural Dynamics* **43**(2), 181–204. doi:10.1002/eqe.v43.2.

Takeda, T., Sozen, M. A. and Neilsen, N. N. [1970] "Reinforced concrete response to simulated earthquakes," *Journal of the Structural Division, ASCE*, **96**, 2557–2573.

Whittaker, A., Deierlein, G. G., Hooper, J. and Merovich, A. (2004). ATC-58 project task report: Engineering demand parameters for structural framing systems. Prepared for the Applied Technology Council by the ATC-58 Structural Performance Products Team. USA.

Wilson, E. L. [1996] *Three-Dimensional Static and Dynamic Analysis of Structures*, Computers and Structures, Inc., Berkeley, CA.

Yuen, Y. P. and Kuang, J. S. [2015] "Nonlinear seismic responses and lateral force transfer mechanisms of RC frames with different infill configurations," *Engineering Structures* **91**, 125–140. doi:10.1016/j.engstruct.2015.02.031.